

IMPACT OF HIGH MEAN TENSILE STRESS ON ALUMINUM STEEL REINFORCED CONDUCTORS FATIGUE LIFE

Aida A. Fadel, aida@unb.br

Jorge Luiz Almeida Ferreira, jorge@unb.br

José Alexander Araújo, alex07@unb.br

Leonardo Brant Murça, leobrantm@hotmail.com

Antonio Manoel Dias Henriques, henriques@unb.br

University of Brasília, Brazil

Abstract. *The aim of this work is to evaluate the effect of a high mean pre-load tensile on the fatigue life of an Ibis steel reinforced aluminum conductor (ACSR) mounted on a monoarticulated cast aluminum suspension clamp. To carry out the tests a new and enhanced version of a fretting fatigue rig for overhead conductors was built. Based on the obtained S-N curves for this assembly it was shown that an increase of the Every Day Stress (EDS) from 20% to 30% of the cable Rated Tensile Strength (RTS) caused an average reduction of 50% in life.*

Keywords: *fretting fatigue, cable fatigue, ACSR conductor, everyday stress.*

1. INTRODUCTION

Mechanical assemblies when subjected to in-field time-variable loading can experience partial slips at contact interfaces, leading to a superficial damage denominated fretting wear (Hills & Nowell, 1994). In particular, the occurrence of high stress gradients close to the contact surfaces can favor the formation, and the initial growth of small cracks, whose subsequent propagation can be accelerated by external cyclic loading, causing the failure by fretting fatigue (Nowell & Araújo, 2001). Experimental evidences show that the combined action of fretting and fatigue have a devastating effect on the fatigue limit of metallic materials (Martins *et al*, 2008), including aluminum alloys (Araújo & Nowel, 2009). Overhead conductors strands fatigue occurs within couplings (e.g. suspension clamps) that restricts the conductor vibration due to vortex induced oscillation (EPRI, 1979; CIGRE, 2008; Azevedo *et al*, 2009; Zou *et al*, 1996), configuring a fretting fatigue mechanical problem. Furthermore, the presence of the axial loading applied to stretch the conductor will facilitate the crack growth.

Transmission lines are designed to sustain mean tensile loads, corresponding to a fraction of the conductor's RTS, the so called EDS, which is one of the main factors at mechanical design of aerial energy lines. EDS setting allows the control of: *i*) sag and consequently minimum safe distance from soil/water surface, *ii*) vibratory behavior and *iii*) levels of static and dynamic stress at the critical points of the structure. Traditionally, transmission lines all over the world have been designed with EDS levels between 15 and 20%. Independently of the conductor stiffness, self-damping and wind velocity (within the aeolian vibration regime) these levels of EDS in the cable seem to keep the bending stress/strain amplitude below maximum allowed values, as recommended by the *Institute of Electrical and Electronic Engineers* (IEEE) and the *Electric Power Research Institute* (EPRI) fatigue design criteria (EPRI, 1979). However, these standard values of bending displacement and stress, which can be endured indefinitely by ACSR conductors, are well known to be excessively cautious (CIGRE, 2007). According to (EPRI, 1979), some preliminary results showed that the EDS level seemed to have little effect on the S-N curves. Conversely, in a recent and comprehensive study carried out by a number of specialists in the subject, published by Cigré (CIGRE, 2008), it was stated that such matter was still not completely set, since "most tests have been conducted at a tension that is representative of the prevailing line conditions", bringing no results for effects of higher EDS levels. Further, Cardou and co-workers (Cardou *et al*, 1994) have attempted to include the cable tension as a conductor fatigue parameter, but results were not conclusive, given that experimental apparatus was not able to keep traction load levels within prescribed tolerance bandwidth during all tests (CIGRE, 2008).

At the design stage, a compromise between the towers heights and/or distances and the conductor's tension, will provide the minimum necessary clearance between the ground and the lowest point of the overhead conductor (Kiessling *et al*, 2003; Fritz, 1960).

Due to the expectations of the Brazilian economy growth for the next two decades, new hydroelectric power plants are being constructed mostly at the Amazon region, where environmental conditions are highly challenging. To provide clearance, and overcome the large spans in the crossing of large and deep rivers (average distance between margins is 1 km and deep 60 m) and also the huge average height of forest is 60 m, new engineering procedures must be developed considering economical and environmental constraints. In such scenario, higher and more robust towers are necessary for installing transmission lines under conventional EDS levels (between 15 and 20% of the cable's RTS), resulting in very expensive projects considering the amount of steel necessary to build such high towers, as well as the amount of space taken by the large towers bases, which will demand significant deforestation. As alternative to reduce the towers height,

smaller spans could be adopted, but in this case, the number of towers and also the number of clearance spots in the forest would increase, bringing no advantage. In this framework, a technical solution that considers an increase in the tension level of the conductor would result in lower towers providing significant economic and environmental savings.

In this setting, in order to provide the sponsors of this research (Eletronorte S.A. and CELG S.A.) a highly important information to the design and maintenance of transmission lines, this work intends to evaluate the fatigue life of an Ibis Aluminum Conductor Steel Reinforced (ACSR), subjected to higher levels of traction load (30% EDS) and compare its fatigue strength performance for tests under the classical EDS loading (around 20% of the Cable RTS). Further, a post mortem analysis of the samples is conducted, in order to generate a mapping of the strand breaking positions inside the clamp and to try to better understand the mechanical variables influencing the phenomenon.

2. TEST PROCEDURE, MATERIALS AND NOMINAL STRESS

2.1. Fretting Rig for Conductors

To carry out tests, two fretting fatigue rigs for overhead conductors were designed (Fadel, 2010). These test apparatus are enhanced versions of a single bench, previously mounted at University of Brasília and described by the authors elsewhere (Azevedo *et al*, 2009), therefore just a brief description will be provided here. Figure 1 depicts a schematic view of such rig. Each fatigue bench is approximately 47 m long. It is divided in active (42 m) and passive (5m) spans. The cable is anchored in a fixed block (at passive span). It is assembled in a monoarticulated suspension clamp attached to a metallic cradle which lays over a moveable concrete block that can be displaced over a 12 m rail track. To simulate the aeolian vibration, an electronically controlled shaker is connected to the cable within the active span. The position of this shaker can be adjusted on a 1.5 m long track. At the right edge of the active span the cable is connected to a lever arm loaded by a dead weight, which stresses the cable. The main objective of this work is to evaluate the impact of this mean stress (EDS) over the assembly's life. Therefore, to make sure the level of mean load in the cable is kept stable during the whole test duration the cable is not clamped at this edge but pass onto a pulley. Further, an actuator is connected to the lever arm and the cable to a load cell so that changes higher than 1% of the prescribed nominal static pre-load are not allowed in the cable.

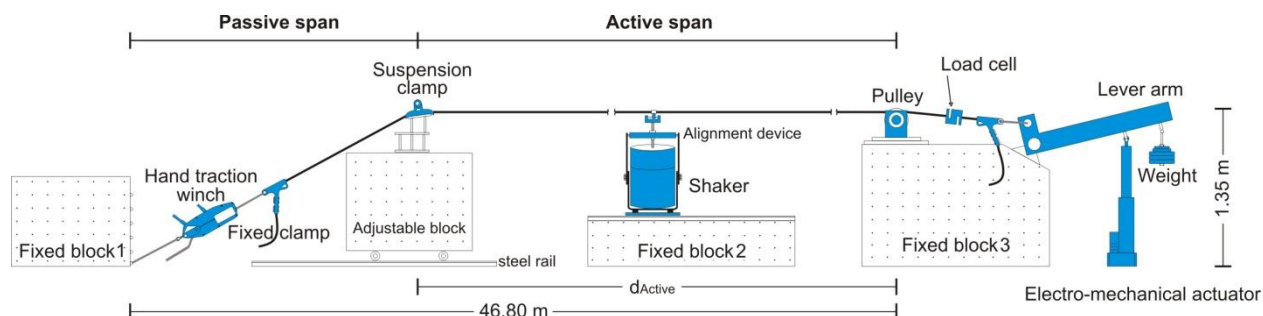


Figure 1- Schematic view of the fretting fatigue rig for overhead conductors.

These new fretting fatigue rigs (Fadel, 2010) have some important modifications with respect to the one first developed in (Azevedo *et al*, 2009). Such changes were necessary as the shaker and its electronic amplifier were systematically breaking during tests. Apparatus adjustments will be described here, in more detail, as the information can be useful for other researchers interested in carrying out this type of experiment. Usually electronically controlled shakers are extremely sensitive to misalignments and side loads. Although extreme care was taken to position the shaker on its trail and connect it to the cable in order to minimize misalignments, temperature variations and creep could still provoke small changes in cable length. As the cable was attached to the shaker by a metallic ring screwed to a bar (Fig. 2a-A), which could freely rotate with respect to the shaker, even small variations in the ring's position could deliver severe lateral loads to the shaker (Fig. 2a-B). We believe these side loads were the main factors damaging the shaker. To correct this problem a new connection device was designed (Fig. 2b) based on a moveable xy table, so that the ring/cable attachment point could move longitudinally and transversally to the cable without transferring side loads to the shaker. This xy table was connected to the shaker by a bar, which was carefully aligned to the center of the shaker. This bar can not move sideways as it passes through a slide bearing mounted on a robust armature attached to the shaker trunion, avoiding lateral loads to reach the field bobine. To provide further protection to the system and to increase the quality and repeatability of the tests, the laboratory environment was conditioned (tests are performed at $20 \pm 1^\circ\text{C}$) and an isolator transformer installed to provide electrical stability. Shakers in both rigs have not failed or presented any other problems since these modifications were implemented in the laboratory, and tests have shown higher stability since then.

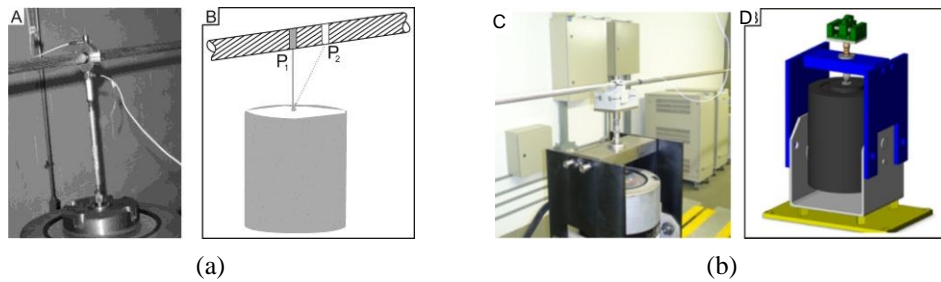


Figure 2- (a) Old connection device (A-Photo of previous cable/shaker connection system and , B-illustration of possible misalignment as connection point displaces from point P1 to P2), (b) New connection device (C-Photo of the new alignment device designed for cable/shaker connection system and , D-schematic drawing of such device).

2.2. Materials and test procedure

Tests have been carried out on an ACSR Ibis conductor sample, with nominal diameter of 19.88 mm. It is made of two 1350-H19 aluminum alloy layers (16 wires in the outer and 10 wires in the inner layer) wrapped on a steel core (7 strands), Fig. 3(A). Aluminum and steel wires diameters are respectively 3.139 mm and 2.441 mm. The cable's RTS is 72.51 kN (7.28 ton). The lower and upper parts of the suspension clamp are made of a high strength (corrosion resistant), non-magnetic cast aluminum alloy with 68.6 kN RTS. The suspension clamp is smooth and uniform, have no sharp edges and its "mouth" has a maximum output angle of 20° in order to prevent damage to the cables (Fig. 3(B)). The system is locked by a 50 N·m torque applied to the nuts that fix the assembly with a pair of U-bolts. Before activating the locking system, a set of wedges is adjusted beneath the plate where the suspension clamp lies on (Fig 3(C)). The aim of these wedges is to simulate the sag angle between cable and clamp in field. For these tests the specified sag angle was 10°. Figure 3(D) shows a sample of the conductor with the lower and upper parts of the suspension clamp and a cross-section view of the cable/clamp assembly.

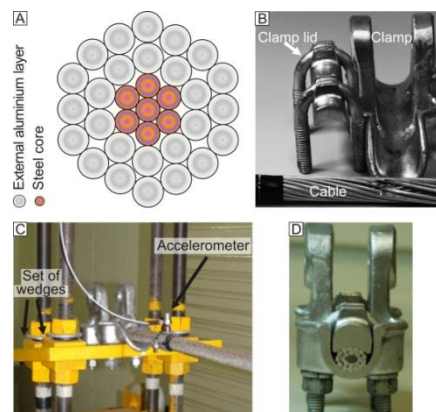


Figure 3 – Photographs of: (A) Ibis conductor composition; (B) Cable and suspension clamp components; (C) Cable/clamp assembly and wedges used to adjust the sag angle; (D) Cutaway view of the cable/clamp assembly.

Test procedure starts by setting the same vertical positions for the suspension clamp and the pulley (in the right hand side of the bench). Next, the dead weight is loaded to tension the cable with a value corresponding to a fraction of the cable RTS (in this case 20 or 30% of the RTS) and the system is left unclamped for 6 h to allow accommodation (IEEE, 2007). Following, the clamp locking system is activated and the controller of the lever arm actuator is adjusted to maintain the load within a $\pm 1\%$ of its nominal value (see Fig. 4).



Figure 4 – Actuator connected to the lever arm in order to maintain the mean stress level in the cable within a $\pm 1\%$ of its nominal value.

The test is controlled in a closed loop by a prescribed displacement, Y_b , measured by a PCB accelerometer positioned at 89 mm from the last point of contact (LPC) between cable and clamp (Fig. 5). Uncertainty in the displacement amplitude, Y_b , is smaller than 0.01 mm. For each fatigue test, frequency of vibration is defined through the application of a previous frequency sweep procedure in which a transfer function is defined by the ratio of displacement, Y_b , and the imposed displacement at the shaker, Y_{shaker} , measured by another PCB accelerometer placed at the top of the connection point between cable and shaker (see Fig. 2(A)).

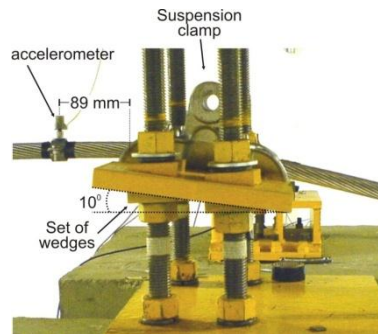


Figure 5 – Location of PCB accelerometer used to control the fatigue test.

Despite the high number of conductor's natural frequencies (Kießling *et al*, 2003) verified by the sweep procedure (an average of 2,0 Hz between the resonant frequencies), just some vibrations modes will guarantee that the power limit of the shaker will not be reached and that only vertical vibration will occur in the active span, as desired. The appropriate mode frequency is then chosen as high as possible to reduce test duration. Typical frequencies are located between 18 and 35 Hz. Figure 6 shows an stable vibratory behavior of conductor under controlled displacement in the neighborhood of a resonant frequency. Tests are interrupted after three aluminum wire breaks (CIGRE, 2008; IEEE, 2007).

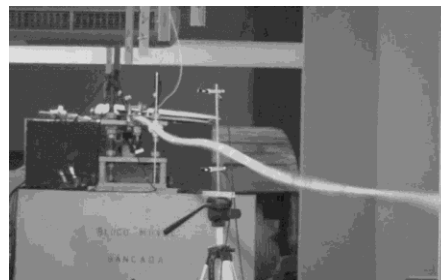


Figure 6 – Stable vibratory behavior of conductor under controlled displacement in the neighborhood of a resonant frequency.

To detect each wire fail, a rotation sensor is positioned at the first node (zero vertical displacement) from the suspension clamp. This sensor is composed by an aluminum blade, which is fastened to the cable by means of a hose clamp. Two laser sensors measure the displacements at each edge of this blade (Fig. 7) and when a wire breaks, the cable rotates due to a redistribution of the tangential component of the force among the remaining strands. The displacements in opposite directions at each edge of the blade are measured by the sensors and recorded by a signal acquisition system. At each event the number of cycles is registered. As the aluminum layers of the cable are wrapped in opposite directions this device is also capable of identifying the layer where the strand breaks. At the end of each test the cable's sample, within the clamp, is removed, not only to make sure that the number and layer of strand failures registered by the rotation sensor is correct.

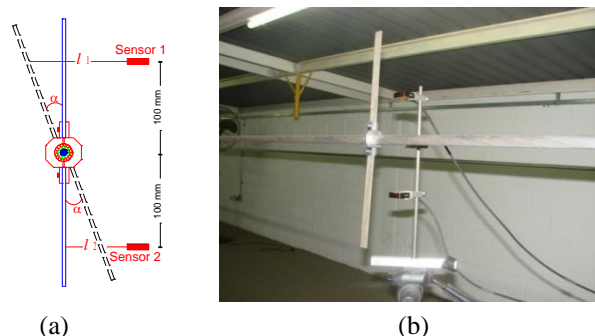


Figure 7 – Rotation sensor for strand failure detection: (a) schematic illustration, (b) photo.

Before cutting the sample, the clamp's mouth position and the 89 mm point are identified on the cable in the active span by a black tape. The upper and lower parts of the suspension clamp, the U-bolts and the nuts are also identified with respect to the span (active or passive) and sides (right or left, looking from the active to the passive span) they are located at. The clamp is then opened and the tension in the cable is unloaded to finally cut out the sample.

2.3. Nominal stress amplitude

Fatigue of conductor strands takes place within fittings that restrain conductor motion due to aeolian vibration, and therefore provokes oscillatory bending stresses. The suspension clamp is a critical device in this setting as it imposes a severe constraint in the vertical direction due to its rigidity. Therefore, the computation of a nominal idealized stress in an aluminum wire close to the clamp mouth is an important parameter that can be related to laboratory fatigue tests results under the same stress level.

In this setting, the Poffenberger-Swart (P-S) formula have been widely used (Poffenberger & Swart, 1965). It relates bending amplitudes, measured at a reference distance from the fixing, to stresses in an aluminum wire of the conductor outer layer. Expression is based on Bernoulli-Euler beam theory and assumes that the conductor works as a fixed cantilever beam under tension with a prescribed vertical displacement at the free edge (Fig. 8).

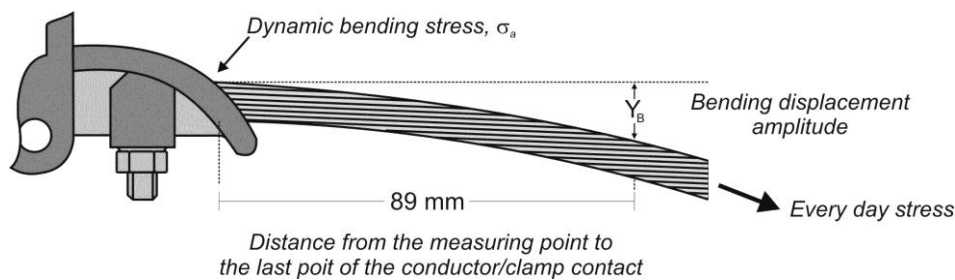


Figure 8 – Scheme of the suspension clamp/cable fixing showing the position where the vertical bending displacement amplitude, Y_b , is measured (89 mm from the last point of contact between cable and suspension clamp).

More specifically P-S formula can be written as:

$$\sigma_a = KY_b, \quad (1)$$

where σ_a is the dynamic bending stress amplitude (zero to peak), Y_b is the conductor's vertical displacement range (peak to peak), measured at 89 mm from the last point of contact (LPC) between cable and clamp, and the Poffenberger parameter, K , is given by

$$K = \frac{E_a d p^2}{4(e^{-px} - 1 + px)} [N/mm^3], \quad (2)$$

being E_a [MPa] and d [mm] the Young's modulus and the diameter of an aluminum wire in the outer layer, respectively. x is the distance on the cable between the last point of contact between cable and clamp and the vertical displacement measuring point (usually $x = 89$ mm) (Fig. 8).

$$p = \sqrt{\frac{T}{EI}}, \quad (3)$$

where T (N) is the static conductor tension (everyday stress, EDS) at average ambient temperature during test period and, EI (N.mm²) is the flexural stiffness of the cable, whose minimum value is:

$$EI_{\min} = n_a E_a \frac{\pi d_a^4}{64} + n_s E_s \frac{\pi d_s^4}{64}, \quad (4)$$

n_a , d_a , E_a are the number, individual diameter and Young's modulus of the aluminum wires and n_s , d_s , E_s are the respective values for the steel wires. In this approach, the conductor is considered as a bundle of individual wires free to move relatively to each other and flexural stiffness takes its minimum value EI_{\min} . For smaller bending amplitudes, the individual strands would stick together thus the conductor would behave as a solid rod, increasing the flexural stiffness to its maximum. Formulae that consider the stick-slip theory to compute EI and hence the dynamic bending stress were proposed elsewhere (Papailiou, 1995; Papailiou, 1997) but will not be addressed in this work.

3. RESULTS

3.1. S-N data

In this work Wöhler (S-N) curves were obtained for two different levels of EDS: 20% (14,5kN) and 30% (22,75kN) of the cable RTS (72,51 kN). As stated before, an EDS equivalent to 20% of the RTS is the usual value adopted by utilities to design transmission lines. Independently of the conductor stiffness, self-damping and wind velocity (within the aeolian vibration regime) this level of mean stress in the cable seems to keep bending strain/stress amplitude in the aluminum wire (of the external layer) diametrically opposite to the last point of contact between cable and suspension clamp, simultaneously under the 150 μ s (peak to peak) limit bending strain amplitude recommended by IEEE (EPRI,1979) and under the 8.5MPa fatigue limit suggested by EPRI (EPRI, 1979) for ACSR multi-layer conductors. A number of lines designed under such preload have operated in Brazil for more than 30 years without presenting significant fatigue problems.

Additionally, it is recognized that either the IEEE or the EPRI criteria provide safe, but extremely conservative values to design overhead conductors against fatigue (CIGRE, 2008), hence at this work tests under a higher mean stress level equivalent to 30% of the cable's RTS were programmed in agreement with design engineers from the Brazilian utilities which sponsor this research (Eletronorte S.A. and CELG S.A.). This value was chosen as it represents a significant increase (50%) on the standard design mean load, which, depending on the fatigue response of the conductor, may lead to a significant reduction of costs by decreasing towers size and the amount of cable necessary to lay the transmission line, especially in the case of large river crossings. EDS values higher than 30% of the RTS were not considered as they seem unrealistic. Calculations made by the utilities engineers show that the level of self-damping for some cables may be significantly reduced for such mean stress values, hence provoking severe vibration of the cable. Furthermore, there are maximum rupture load criteria for unexpected wind loads (usually 60 to 70% of the cable's RTS) that can be violated if much higher values than the 30% EDS here suggested are considered.

A total of 35 fatigue tests were carried out at the middle high cycle fatigue regime, being 19 samples stretched by loads corresponding to 20% cable's RTS (20% EDS) and other 16 samples tested under 30% cable's RTS (30% EDS) (Fadel, 2010). Again, the sag angle was 10°, and the clamping pressure was generated by applying a 50 N.m torque to the locking system.

The P-S formula (Eq. 1) establishes a relation between amplitude of displacement and stress amplitude. Therefore, for sake of comparison, at each level of EDS, tests¹ were planned to run either under (i) the same nominal stress amplitude (different amplitude of displacement, Y_b) or under, (ii) the same prescribed amplitude of displacement Y_b (different nominal stress), as reported in Table 1 (columns filled in grey report parameters corresponding to tests (i)). Here it is important to emphasize that, although all tests were conducted under displacement control, as detailed in section 2.2, it is possible to run different tests under the same nominal stress amplitude by invoking the P-S formula to determine the corresponding levels of displacement, Y_b , used to control the test.

Table 1 – Nominal stress and corresponding displacement amplitudes prescribed in the fatigue tests.

Nominal Stress, σ_a [MPa]	25.08	28.22	31.35	34.49	35.87	39.83	43.31	
Y_b , [mm]	20% EDS	0.8	0.9	1.00	1.1	-	1.27	1.38
	30% EDS	0.7	-	0.87	0.96	1.0	1.11	1.21

Tables 2 and 3 report the peak-to-peak vertical displacements, Y_b , prescribed at 89 mm from the LPC; the bending stress amplitude at an aluminum wire (diametrically opposite to the LPC) of the external layer (0 to peak), σ_a , given by the P-S formula; the total number of strand breaks in each test²; test duration and the number of cycles required to break the first, second and third aluminum wires. Figures 9 (A) and 9 (B) depict the response of the rotation sensor indicating the instants of each wire failure and the corresponding cables' sample, respectively, for a test where the cable was under an EDS=20% of the cable's RTS, $Y_b=1$ mm and test lasted for 4.66 x 10⁶ cycles (see Table 2). The occurrence of all rotations in the same direction indicates that strands break happened to the same layer (in this case in the external one), as can be confirmed by the sample's *post mortem* inspection (see Figure 9(B)). Notice in this same figure that, the distance between the clamp mouth and accelerometer (68.5 mm) does not correspond to the distance between the LPC and the accelerometer (89 mm). The clamp mouth is adopted as a useful reference point to measure the position of wire failure within the clamp.

¹For some test conditions, it was not possible to achieve a controllable/stable test under the same bending displacement amplitude. In these cases, the test was set to run at a displacement amplitude as close as possible from the value prescribed for the test under a different mean tension in the cable, as can be seen in Table 1.

²Tests were not automatically stopped at third wire break but after analysis of the rotation sensor acquired signal. For initial tests at each displacement level calibration of the system sometimes required us to interrupt the test before three wires broken. In other cases, the data analysis was performed after a later stage in the test when more than three aluminum wires were broken.

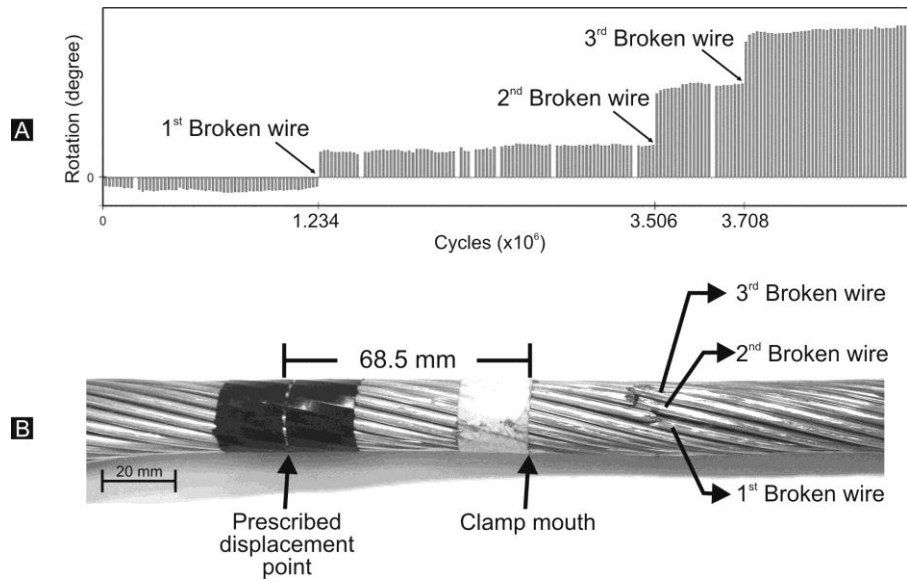


Figure 9 – (A) Response of rotation sensor for a test under $Y_b=1\text{mm}$ and $\text{EDS}=20\%$ of RTS (Test duration was 4.66×10^6 cycles). (B) Analysis of cable's sample for this same test showing three wire breaks at the external layer.

Table 2 – Test parameters and results for EDS corresponding to 20% of cable's RTS.

Y_B [mm]	σ_a P-S [MPa]	Number of Breaks	Test Duration $N \times 10^6$ [cycles]	1 st Break	2 nd Break	3 rd Break	
				$N \times 10^6$ [cycles]	$N \times 10^6$ [cycles]	$N \times 10^6$ [cycles]	
0.80	25.08	0	25.00	> 25			
		1	5.50	5.50	> 5,5	> 5,5	
		2	9.03	2.98	6.34	>9,03	
		4	5.73	3.00	3.42	4.50	
		4	9.32	1.90	7.44	9.10	
		Mean		3.35	5.73	6.80	
		Standard Deviation		1.53	2.08	3.25	
1.00	31.35	1	3.90	3.10	>3,9	>3,9	
		6	4.66	1.24	3.51	3.71	
		3	7.40	3.57	5.81	7.30	
		5	9.00	1.36	2.73	5.74	
		5	10.58	3.10	4.30	7.10	
			Mean		2.47	4.09	5.96
	Standard Deviation		1.09	1.32	1.65		
1.10	34.49	4+2T	3.20	0.98	2.45	2.49	
		2 ½	4.31	-	-	4.31	
		6 ½	5.28	1.77	2.46	3.15	
		5 ½	6.13	0.64	1.07	1.84	
		3	6.27	-	-	6.27	
			Mean		1.13	1.99	3.61
	Standard Deviation		0.58	0.80	1.74		
1.27	39.82	4	2.00	0.99	1.47	1.64	
		3	2.45	1.01	1.42	2.31	
			Mean		1.00	1.45	1.98
			Standard Deviation		0.02	0.04	0.47
1.38	43.31	5	0.98	0.42	1.05	1.19	
		4¾	1.23	0.65	0.73	1.05	
			Mean		0.53	0.89	1.12
			Standard Deviation		0.17	0.23	0.10

Table 3 – Test parameters and results for EDS corresponding to 30% of cable’s RTS.

Y_B [mm]	σ_a P-S [MPa]	Number of Breaks	Test Duration $N \times 10^6$ [cycles]	1 st Break	2 nd Break	3 rd Break
				$N \times 10^6$ [cycles]	$N \times 10^6$ [cycles]	$N \times 10^6$ [cycles]
0.70	25.08	3	15.00	3.29	4.20	15.00
		3	2.97	1.45	1.45	2.79
0.87	31.35	3	3.75	1.30	1.98	2.90
		9	6.57	0.93	1.65	1.65
		Mean		1.12	1.82	2.28
		Standard Deviation		0.26	0.23	0.88
0.96	34.49	2	1.75	1.27	1.39	-
		3	1.78	0.69	0.91	0.99
		4	2.54	1.13	1.34	2.10
		7	3.18	0.70	1.13	2.31
1.00	35.87	4	3.50	1.12	1.45	1.82
		6	3.52	0.89	1.21	1.30
		Mean		0.91	1.21	1.70
		Standard Deviation		0.21	0.21	0.55
1.10	39.83	3	1.61	0.56	1.3	1.61
		5	2.10	0.74	0.99	1.29
		Mean		0.65	1.14	1.45
		Standard Deviation		0.13	0.22	0.22
1.21	43.31	3	1.10	0.28	0.92	0.98
		4	1.46	0.84	0.87	1.02
		4	1.50	1.00	1.16	1.36
		4	1.80	0.66	1.09	1.30
Mean		0.69	1.01	1.17		
Standard Deviation		0.31	0.14	0.19		

From the generated experimental data S-N curves were plotted for this cable/clamp arrangement for mean tensile of 20% and 30% of the EDS, as depicted in Fig. 10. Such graph also contains the Cigré Safe Border Line (CSBL) (CIGRE, 1995) which corresponds to a S-N based on aluminum wires and cables fatigue tests under laboratory conditions. It represents a lower bound limit for the admissible number of cycles that, aluminum, aluminum alloys and multilayer ACSR conductors, mounted on different types of clamps, can sustain without failure under various stress levels. A qualitative analysis of experimental S-N curves (Fig.10) revealed that, for the cable/suspension clamp configuration tested the fatigue life is significantly affected by the increase in the EDS level, mainly for stress amplitudes lower than 35 MPa.

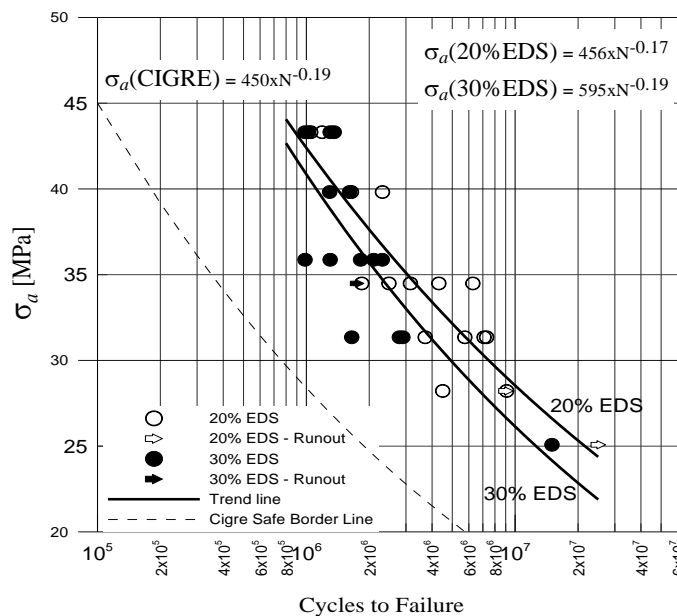


Figure 10 – Cigré’s Safe Border Line and S-N experimental data for IBIS ACSR conductor considering EDS=20% and 30% of RTS. Tests were interrupted at third aluminum wire break.

On the other hand, it seems clear that, for stress levels higher than these, such effect of the mean stress on the fatigue life tends to be reduced. To quantify these trends Table 4 reports the ratio between the average life for tensions of 30% and 20% of the cable's RTS, which was 0.38 for a low stress amplitude such as 31.35 MPa, then increased to 0.73 and to 1.04 for stress amplitudes of 39.83 and 43.41 MPa, respectively. Also in Table 4, it is possible to compare the life ratio between the experimental data under both EDS levels to the life estimated by the Cigré Safe Border Line. Note that CSBL estimates lives about 3 to 11 times lower than the ones verified by the experimental tests.

Table 4 – Life ratio for the average number of cycles to 3th wire break at the same stress amplitude for 30% and 20% EDS.

EDS	σ_a [MPa]		
	31.35	39.83	43.31
20%	5.96	1.98	1.12
30%	2.28	1.45	1.17
CSBL	0.61	0.18	0.12
$N_{30\% \text{ EDS}}/N_{20\% \text{ EDS}}$	0.4	0.7	1.0

4. DISCUSSION OF RESULTS

This work was essentially of experimental nature. The main purpose was to investigate how an increase in the mean tensile stress applied to lay overhead conductors, the so called cable EDS, affected its fatigue life in the medium high cycle fatigue regime. As a whole, results showed that an increase of 50% in the traditional value of mean load (corresponding to around 20% of the cable's RTS), caused a significant reduction in the fatigue life of an Ibis ACSR conductor for stress amplitudes varying from 25 to 43MPa. To be precise, such effect was more pronounced at low stress amplitudes, and tended to disappear at high stress levels. Within the aeolian vibration regime the displacement amplitudes are usually smaller than 1 mm, i.e., low stress amplitudes prevail. Therefore, care must be exercised by the design engineers should higher levels of EDS be required to reduce line costs, or to trespass logistic problems, such as building huge transmission line towers in the middle of the Amazon forest in order to cross large rivers. This choice is further complicated by the fact that the fatigue loading increases with EDS level, since less self-damping occurs among wires under higher levels of preload. Notice that, partial slip is a contact regime associated with very small relative displacements and corresponds to high radial load on the conductor and high normal load at the contact points, causing fretting wear. This mixed fretting regime is the most critical with respect to fatigue crack initiation (Hills, D.A. & Nowell, 1994; Araújo *et al* 2008; Zou *et al*, 1992; Zou *et al*, 1997).

On the other hand, the available fatigue criteria suggested by IEEE and EPRI, which recommend that the time varying bending strain on the external aluminum strand at the LPC must be in the range of 150 to 300 μ s to guarantee that the cable will endure indefinitely, do not define how far such strain/stress levels are from the cable real fatigue limit. In this setting, there is room to enhance design approaches against fatigue in these mechanical structures. The raise of S-N curves under laboratory conditions becomes hence an important tool to define new design limits. Not only the effect of the EDS on the fatigue strength can be determined by this mean but also the impact of other local important variables to the phenomenon, such as the torque applied to the locking system.

In the case of overhead conductors the fatigue inducing stresses at the contact between individual wires or between the external wires and the clamp surface are not accessible to direct measurement and their estimation by any sort of numerical procedure is not an easy task either due to the complexities involved in inner conductor mechanics (plasticity, variable flexural stiffness and wear resulting from partial slip contact regime, etc) (Papailiou, 1997). Therefore, the effect of variables, such as the clamping pressure, on cable's fatigue durability can be implicitly detected by the nominal stress computed according to the P-S (Poffenberger & Swart, 1965) if tests are carried out.

Failure analysis revealed that cracks always initiated in fretted areas at wire/wire or wire/suspension clamp contact regions. Wire breaks were located within clamps in regions where, without opening the suspension clamp, visual inspection is not possible. As a higher number of strands broke at the bottom part of the external layer, line men from the utilities maintenance sectors, need not only to open clamps but also to raise the cable from the clamp cradle to detect the damage.

5. CONCLUSION

The following conclusions can be drawn from this work:

- The increase of the mean tensile stress applied to the cable, i.e. the EDS, from 20% to 30% of the Ibis ACSR RTS provoked an average reduction of 50% in the conductors fatigue life. This reduction was especially significant at low stress amplitudes typical from aeolian vibration. At high stress amplitudes such effect was very mild;
- Cigré's Safe Border Line S-N curve, which is commonly adopted as reference for design and maintenance procedures by transmission line engineers, revealed to be an extremely conservative tool;

- Failure analysis indicated that the increase in EDS level from 20 to 30% of cable's RTS generated a change in the distribution of the broken wires among the internal and external aluminum layers. At the higher mean load there were twice more strand breaks in the external layer than in the internal one;

6. ACKNOWLEDGEMENTS

The financial supports of ELETRONORTE S.A., CELG S.A., CNPq, CAPES, Finatec are gratefully acknowledged.

7. REFERENCES

- Araújo, J. A.; Susmel, L.; Taylor, D.; Ferro, J.C.T. ; Ferreira, J. L.A. , 2008, "On the prediction of high cycle fretting fatigue strength, theory of critical distances vs. hot spot approach". *Engineering Fracture Mechanics*, v. 75, p. 1763-1778.
- Araújo, J. A. and Nowell, D., 2009, "Mixed High Low Fretting Fatigue of Ti 6/4: Tests and Modelling", *Tribology International*, v. 42, p.1276-1285.
- Azevedo, C.R.F., Henriques, A.M.D., Pulino Filho, A.R., Ferreira, J.L.A. and Araújo, J.A., 2009, "Fretting fatigue in overhead conductors: Rig design and failure analysis of a Grosbeak aluminium cable steel reinforced conductor". *Engineering Failure Analysis* 16, pp. 136–151.
- Cardou, A., Leblond, A., Goudreau, S., Cloutier, L., 1994, "Electrical Conductor Bending Fatigue at Suspension Clamp: a Fretting Fatigue Problem", *Fretting Fatigue*, ESIS 18, Mechanical Engineering Publications, London, pp. 257-266.
- CIGRE, 1985, SC22-WG04. "Guide for Endurance Tests of Conductors inside Clamps", *Electra*, No 100, May, pp. 77-86.
- CIGRE ,1995, SC21-WG11. *Fatigue Endurance Capability of Conductor/Clamp Systems-Update of Present Knowledge*. TB # 332, Paris, 2007.
- CIGRE, 2007, SCB2-WG11-TEZ. "Guide to Vibration Measurement on Overhead Line". *Electra* n° 163, December.
- CIGRE, 2008, SCB2-08-WG30-TF7. "Engineering Guidelines Relating to Fatigue Endurance Capability of Conductor/Clamp Systems".
- EPRI, 1979, "Transmission Line Reference Book: The Orange Book". Electric Power Research Institute. Palo Alto,CA.
- Fadel, A. A., 2010, "Avaliação do Efeito de Tracionamento em Elevados Níveis de EDS Sobre a Resistência em Fadiga do Condutor IBIS (CAA 397,5 MCM)". Doctorate Thesis, University of Brasília, DF, Brazil, 185 p.155:317–30.
- Fritz, E., 1960, "Effect of Tighter Conductor Tensions on Transmission Costs", AIE: Winter General Meeting, New York.
- Hills, D.A. & Nowell, D. ; 1994, "Mechanics of fretting fatigue". Dordrecht: Kluwer Academic publishers.
- IEEE Std 563, 2007, "Guide for Endurance Tests of Conductors Inside Clamps", *ELECTRA* No 100, May (R2007), pp.77-86.
- Kiessling, F., Nefzger, P., Nolasco, J.F., Kaintzyk, U., 2003, "Overhead Power Lines: Planning, Design, Construction", Springer-Verlag, Berlin, Heidelberg.
- Martins, L. H. L.; Rossino, L. S. ; Filho, W. W. B.; Araújo, J. A, 2008, "Detailed design of fretting fatigue apparatus and tests on 7050-T7451 Al alloy",*Tribology – Materials, Surfaces & Interfaces* v. 2, p. 39-49.
- Nowell, D.; Araújo, J. A.; 2001, "Application of Multiaxial Fatigue Parameters to Fretting Contacts with High Stress Gradients". In: *Third International Symposium on Fretting Fatigue*, 2001, Nagaoka-shi. *Fretting Fatigue*, v. 1.
- Papailiou, K. O., 1995, Improved calculations of dynamic conductor bending stresses using a variable bending stiffness. *CIGRE*, SC 22 WG11. Madrid Oct; paper 22-95(WG 11)-138.
- Papailiou, K. O., 1997, "On the bending stiffness of Transmission Line Conductors". *IEEE Transactions on Power Delivery*. 12: 1576-1588.
- Poffenberger, J. C., Swart, R.L., 1965, "Differential displacement and dynamic conductor strain". *IEEE Transactions PAS-84*: 281-289.
- Zhou, Z.R., Fayeulle, S., Vincent, L., 1992, "Cracking behaviour of various aluminium alloys during fretting wear". *Wear*.
- Zhou, Z.R., Cardou, A., Fiset, M., Goudreau, S., 1994, "Fretting fatigue in electrical transmission lines", *Wear*, 173, pp. 179-188.
- Zhou, Z.R., Cardou, A., Goudreau, S., Fiset, M., 1996, "Fundamental investigations of electrical conductor fretting fatigue", *Tribology International*, Vol. 29, No 3, May pp. 221-232.
- Zhou, Z.R., Gu, S.R., Vicent, L., 1997, "An investigation of the fretting wear of two aluminium alloys". *Tribol. Int*;30:1–7.

5. RESPONSIBILITY NOTICE

The authors are the only responsible for the printed material included in this paper.